

***Rhazya stricta*- Biosynthesized Copper Nanoparticles on
Staphylococcus aureus Infected Rabbit Wounds**

**Ali Hussein Aldujaily¹, Kifah Fadhil Hassoon², Douaa Barzan Salman¹, Ghadeer Sabah
Bustani³**

¹Department of Veterinary Clinical Sciences, Faculty of Veterinary Medicine, University of Kufa, Iraq.

²Department of Veterinary Microbiology, Faculty of Veterinary Medicine, University of Kufa, Iraq.

³The Islamic University, Najaf, Iraq

Abstract

BACKGROUND: Nanoparticles are utilized in various technological fields, including medicine, due to their inherent antibacterial properties. Recent research has focused on the biosynthesis of copper nanoparticles (CuNPs) and their potential medical applications.

OBJECTIVE This study aimed to use *Rhazya stricta* for the green synthesis of CuNPs and assess their effectiveness in eradicating bacterial pathogens, particularly *S. aureus*, and promoting wound healing in rabbits.

MATERIAL AND METHODS The synthesized nanoparticles were characterized using UV-visible spectroscopy, scanning electron microscopy (SEM), Energy Dispersive Spectroscopy (EDS), X-ray diffraction (XRD), atomic force microscopy (AFM), and Zeta potential analysis. Fifteen rabbits were divided into three groups of five. Full-thickness costo-abdominal skin wounds were created on the right side of each rabbit. The first group served as the untreated control, the second group was treated with CuNPs, and the third group received fusidic acid treatment.

RESULTS: *R. stricta* extract successfully synthesized CuNPs. The application of CuNPs on *S. aureus*-contaminated wounds showed faster healing than fusidic acid treatment. The CuNPs group healed in 16 days, while the fusidic acid group healed in 22 days. CuNPs-treated wounds had significantly reduced wound area, total cell count, neutrophil count, macrophage count, and lymphocyte count ($P < 0.05$), along with increased wound contracture ($P < 0.05$). Bacterial counts indicated that CuNPs eradicated *S. aureus* infections in 7 days, compared to 12 days for fusidic acid. CuNPs reduced inflammation and promoted collagen fiber deposition, leading to better healing of *S. aureus*-infected wounds by decreasing hemorrhagic regions and inflammatory cells.

Conclusion: CuNPs synthesized using *R. stricta* show promising potential as a safe and effective treatment for infected wounds. They effectively eradicate infections and promote efficient wound healing, making them a viable therapeutic option for managing infected wounds.

Keywords: *Rhazya stricta*, Copper nanoparticles, *Staphylococcus aureus*, Skin wounds, Histopathology, Rabbits.

Introduction

The process of wound healing is a multifaceted and intricate reaction that involves various stages, such as platelet accumulation, coagulation, inflammatory response to injury, modification of the underlying materials, angiogenesis, and re-epithelization (Huimin et al., 2023). The presence of pathogens in a wound can impede the healing process and increase the risk of sepsis, a serious medical condition. Chronic wounds provide an optimal environment for the development of mature biofilms, which offer bacteria protection against the impact of antibiotics and the body's immune proteins (Razdan et al., 2022; Bustani and Kashef Alghetaa, 2024).

The bacterium *Staphylococcus aureus*, commonly referred to as *S. aureus*, has been recognized as a prominent etiological agent responsible for wound infections. This pathogen possesses the capacity to acquire resistance to multiple antibiotics, thereby exacerbating the challenge of effectively treating chronic infections (Foroutan et al., 2022; Pal et al., 2023).

The utilization of nanotechnology in the field of medicine is increasingly prevalent, leading to its application in addressing the challenge of antibiotic resistance. Bioactive nanoparticles (NPs) are a prominent category of nanomaterials that are being explored for

potential clinical applications. These NPs possess several advantageous characteristics, including cost-effectiveness, a significant surface -to- volume ratio, exceptional stability, and a high level of safety (Samuel et al., 2022; Hossieni et al., 2024).

Copper nanoparticles (CuNPs) have garnered significant attention due to their diverse range of applications, including their use as antibacterial and antifungal agents, as well as their antioxidant properties and ability to prevent biofilm formation in the fields of biotechnology and bioengineering (Zhang et al., 2022). The CuNPs can be synthesized through diverse methodologies, encompassing physical, chemical, and biological approaches. Biological environmentally friendly approaches are preferred over alternative methods (Hasanin et al., 2021).

The selection of plant materials for biosynthesis is based on the presence of reducing agents such as ascorbic acid and phenolic compounds, which have been identified as potentially important factors in the synthesis of metal nanoparticles (Islam et al., 2022). Existing literature indicates that *R. stricta* exhibits a significant abundance of diverse phytoconstituents, encompassing flavonoids, steroids, tannins, saponins, glycosides, terpenoids, coumarins, and beta-cyanins. The literature has documented that these phytoconstituents exhibit diverse pharmacological activities, including antioxidant, anti-inflammatory, and anti-cancer properties (Rahman et al., 2023; Rahchamani et al., 2024).

Numerous studies conducted in recent years have established the efficacy of CuNPs as agents for wound healing, offering a protective barrier against infections. CuNPs have been observed to induce angiogenesis, the process of new blood vessel formation, at the site of the wound. In addition to this, CuNPs also induce the upregulation of vascular endothelial growth

factor (VEGF), which promotes the transportation of various nutrients and the formation of collagen, both of which are essential for wound healing (Gaddafi et al., 2023; Yaşayan et al., 2023).

The primary objective of this study was to investigate the effects of CuNPs synthesized by *R. stricta* on surgically induced full thickness skin wounds in rabbits that were intentionally infected with *S. aureus*.

Material and methods

Study Design

The study was conducted in two distinct phases. The initial phase focused on the biosynthesis of CuNPs using *R. stricta*. In the subsequent phase, *S. aureus* was isolated from contaminated wounds of dogs. Following this, skin wounds on rabbits were infected with staphylococci and subsequently treated with CuNPs. The animal's gender was not considered in this investigation because the medication was applied externally to the skin, and there was no observed difference in skin healing between males and females.

Ethical Approval

The current study was carried out in accordance with the guidelines set forth by the Animal Ethics Committee of the Faculty of Veterinary Medicine at the University of Kufa, adhering to the regulations outlined in the granted license (Approval no. 16881 dated 12/7/2023).

Production of CuNPs

Plant Collection.

In this study, the researchers collected the leaves and stem of *R. stricta* from the arid region of Al-Najaf in Iraq. The specimen was collected and verified at the Herbal Center for scientific authentication, located within the Department of Physiology and Pharmacology at the Faculty of Pharmacy, University of Kufa, Iraq.

Plant Extraction.

The leaves of *R. stricta* were collected and subjected to two rounds of washing with distilled water to remove any dust particles. Subsequently, the leaves were air-dried in the shade at room temperature. The dried leaves, weighing 25 grams, were fragmented and introduced into an Erlenmeyer flask containing 250 milliliters of sterile distilled water. The flask was subjected to a temperature of 90 °C in a water bath (Gallen Kamp; England) for 45 minutes. In order to generate the aqueous plant extracts, the extract underwent filtration using Whatman No. 1 filter paper and subsequent centrifugation at a speed of 3000 rpm for 10 minutes (Awwad et al., 2013). In order to ensure the absence of contamination in the prepared extracts, a volume of 0.1 ml of the plant extract was acquired and cultivated on nutrient agar. Subsequently, the agar plates were incubated at a temperature of 37 °C for 24 hours.

Biosynthesis of CuNPs

Following the filtration mentioned above process, 25 ml of each aqueous extract was individually introduced into a 250 ml Erlenmeyer flask containing 100 ml of a 0.01M CuSO₄ solution. This sequential addition was carried out for 10-15 minutes. The flask's contents were agitated using a magnetic stirrer operating at a rotational speed of 150 rpm and maintained at a temperature of 30 °C. The CuNPs production process was deemed complete when a transition in color occurred, shifting from a light-yellow hue to a dark green shade. This change was

attributed to the surface Plasmon resonance phenomenon, which resulted in a peak at the wavelength range of 550-600 nm as observed using a UV-visible spectrophotometer (Shimadzu; Japan). Following this, the sample was subjected to centrifugation at a speed of 6000 rpm for 15 minutes. The resulting supernatant was then discarded and replaced with deionized distilled water. Subsequently, the sample was centrifuged three additional times at the same speed and duration to ensure the complete removal of any remaining supernatant. The resulting pellet was then stored overnight in a hot air oven maintained at a temperature of 60°C. This process ultimately yielded nanoparticle powder, as described by (Rani et al., 2020).

Characterization of CuNPs

The characterization of the samples was conducted using UV-visible spectroscopy. The achievement was accomplished through the evaluation of the UV-visible spectra of the reaction mixture, which underwent periodic dilution with deionized distillation water (Caroling et al., 2013).

The shape and size of the nanoparticles were determined using scanning electron microscopy (SEM) (FEI; Netherland). The X-ray diffraction (XRD) (Broker; Germany) is a widely employed technique for the examination of molecular and crystal morphologies, qualitative identification of chemicals, quantitative determination of chemical species, assessment of crystallinity, analysis of isomorphous replacements, and measurement of particle sizes (W. Zhang et al., 2017).

The presence of nanoparticles in a point analysis was determined using energy-dispersive X-ray spectroscopy (EDS) as described by (Caroling et al., 2013). The study conducted by (Vinelli et al., 2008) examined the dispersion and aggregation of nanomaterials, as well as their size and

form, through the utilization of atomic force microscopy (AFM). The stability of the produced nanoparticles was assessed using a Zeta potential analyzer (Brookhaven; USA), which measured the zeta potential values ranging from -160 mV to +160 mV. The obtained data was then visualized in graphical form (Raja et al., 2017).

Experimental study

Laboratory animal initialization

Fifteen adult domestic rabbits of both sexes (11 male and 4 female) aged 8–10 weeks with an average body weight of $1,800 \text{ g} \pm 20 \text{ g}$ were fed commercial pellets and grass for 7 days prior to the start of the experiment for acclimatization, which was conducted from August 2023 to October 2023 in the animal house of the faculty of Veterinary medicine at the University of Kufa, Iraq. The animals were randomly divided into three equal groups ($n = 5$).

Anesthesia and wounding

The rabbits were anesthetized intramuscularly using a Ketamine-Xylazine-saline solution that contained 40 mg/kg of Ketamine (Holland) and 2 mg/kg of Xylazine (Belgium)(Cardoso et al., 2020). In brief, rabbit hair was removed, and the exposed skin was cleaned with 70% ethanol (APCO; Jordan). 1 cm in diameter full-thickness skin incisions were made on the rabbit's thoracoabdominal side (figure 1). The exposed wounds received no dressings throughout the experiment (Behera et al., 2019).



Figure 1: A rabbit with incisions on its skin

Preparation of bacteria

In the Al-Najaf Teaching Veterinary Hospital, *S. aureus* was isolated from contaminated wounds of dogs. The VITEK-2 (Biomerieux; France) compact automated system was utilized for bacterial identification and antibiogram testing based on the MIC technique determination. Depending on VITEK-2 compact system, Antibiotic Susceptibility Test (AST) was it turns out that isolated bacteria resistant to many classes of antibiotic e.g., benzylpenicillin, oxacillin, Tobramycin, Moxifloxacin, Clindamycin, Vancomycin and Tetracycline. Fusidic acid was selected due to the reduced susceptibility of the *S. aureus* isolate to other antibiotics.

The microorganisms were cultivated in Muller-Hinton broth. After undergoing centrifugation at a speed of 1,000 rpm for 15 minutes, the bacteria were diluted in sterile phosphate-buffered

saline to achieve a concentration of 1×10^8 CFU/ml. Following wound surgery, 100 microliters of bacterial suspension were topically applied to each wound bed (Tanideh et al., 2014).

Experimental Treatments

As mentioned earlier, the rabbits were divided into three distinct groups. There were five animals in each group, and each group administered the prescribed medication five days subsequent to the initiation of infection. All three animal groups were treated in the following manner:

1. Control group: non-treated.
2. CuNPs- treated group: treated with 0.2% CuNPs ointment applied daily for 5 days on the affected skin.
3. Fusidic acid - treated group: treated with 2% Fusidic acid ointment applied daily for 5 days on the affected skin.

Data Collection

Documentation of wound healing time

The duration of wound healing was measured from the moment of wound induction to re-epithelialization. The observations were randomly estimated at intervals of 7, 14, 21, and 28 until the scar had completely disappeared (Mirnezami et al., 2018).

Determination of healing rate

At 7-day intervals, the rate of healing for each treatment group was assessed. It was determined by dividing the highest average wound margin distance from the wound's center by the time required for wound closure. The following formula was used to determine the weekly healing rate:

Wound Closure (%) = [(Area of the wound on day 0 (mm)– area of the wound on indicated day) (mm)] /Area of the wound on day 0 (mm) ×100 (Sato et al., 2015).

Identification of WBC count

The WBC count was conducted using the Vet. Scan HM5 hematology equipment manufactured by ABAXIS Company. The WBC was assessed on a weekly basis for every treatment group.

Histopathological Evaluation

On days 3, 7, 14, and 21 of the experiment, a histological test was done to discriminate between these groups by taking 5 mm of the healing regions. Overnight, the skin slices were fixed in a 10% formalin (BDH; England) solution (pH 7.4). They were then processed through a succession of alcohol and xylene grades. Following that, the tissues were immersed in paraffin wax at 65°C. Tissue blocks were cut into 5µm thick slices, stained with hematoxylin and eosin (H&E), and examined under a light microscope (Al Mousaw et al., 2020; Diniz et al., 2020).

Statistical analysis

Data were investigated using SPSS version 26. The results were presented as mean ± standard errors (SE), and a P value < 0.05 was considered statistically significant. The data were statistically analyzed using the one-way ANOVA.

Results

Copper nanoparticle biosynthesis

Following a 24-hour incubation period, a discernible alteration in color was observed, signifying the occurrence of nanoparticle formation within the reaction mixture. The alteration in

color of the medium was observed as a transition from a yellow hue to a reddish-brown shade upon the introduction of the plant extracts and CuSO₄ reaction mixture, conducted under conditions of darkness (figure 2).



Figure 2: Visualization of the green synthesis of CuNPs. (A) before incubation; (B) a solution containing CuNPs after incubation.

Characterization of CuNPs

UV- Visible Spectroscopy

The confirmation of nanoparticle biosynthesis can be achieved through visual observation and the measurement of the surface plasmon resonance (SPR) band using UV-vis spectroscopy. According to (Badri et al., 2021), the presence of a solitary SPR band suggests that the nanoparticles possess a spherical morphology. The UV-Visible spectrogram, as illustrated in Figure 3, demonstrates the successful synthesis of CuNPs and the presence of their distinctive surface plasmonic resonance peak at a wavelength of 570 nm.

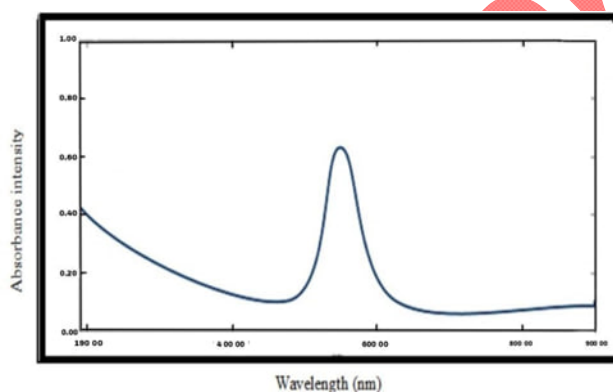


Figure (3): UV-visible spectroscopy analysis of CuNPs synthesis by *Rhazya stricta*

Scanning Electron Microscopy (SEM) Analysis

The SEM was employed to validate the morphology and dimensions of the biogenic nanoparticles (Chinnathambi et al., 2021). This study examines the distribution and morphology of biogenic nanoparticles (NPs) synthesized by *Rhazya stricta*. The CuNPs, which are spherically shaped, exhibit a well-dispersed nature. The average size of these CuNPs is measured to be 15.75 nm (figure 4).

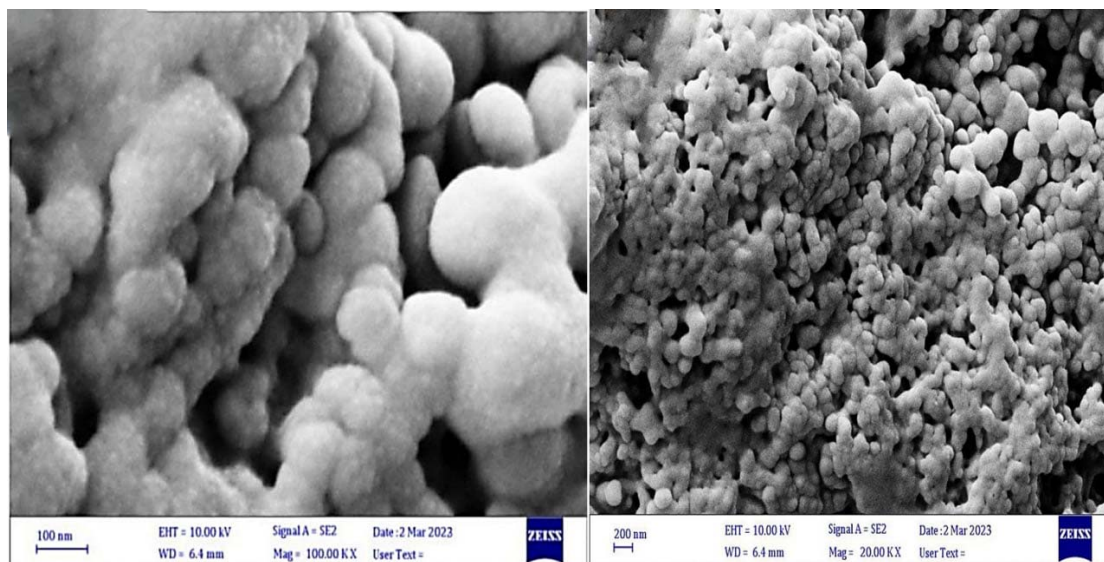
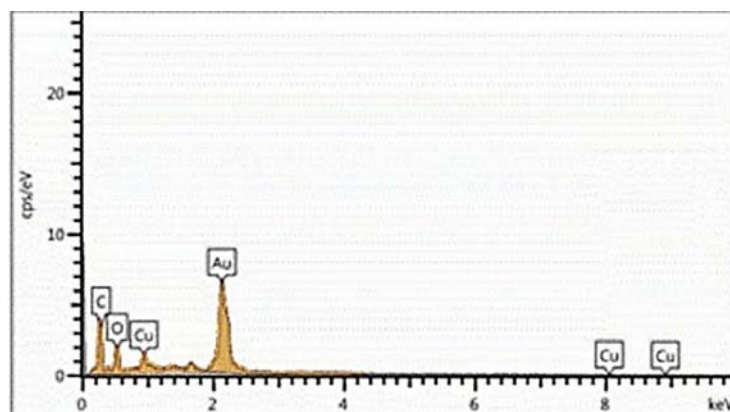


Figure (4): SEM Analysis of NPs synthesis by *Rhazya stricta* taken at different scales.

The SEM images of the CuNPs exhibited an irregular, diminutive spherical morphology. This finding is consistent with the observations reported by (Zhao et al., 2022).

Energy Dispersive Spectroscopy (EDS) Analysis

The EDS technique, specifically point and mapping analysis, was employed to quantitatively assess the presence of NPs by examining the optical absorption peaks of various elements. The elemental analysis of CuNPs synthesized by *R. stricta* revealed the composition of constituent elements, as depicted in Figure 5.



Elements	Wt%
C	55.1
O	23.0
Cu	21.9

Figure (5): EDS Analysis of biogenic nanoparticles synthesized by *R. stricta*

The analysis of EDS spectroscopy was conducted on CuNPs synthesized using *R. stricta*, thereby validating the existence of elemental copper through the observed signals. The EDS spectrum exhibited a discernible peak, attributed to the absorption of copper nano crystallites that correspond to SPR. The observed component was copper, and additional elements, such as oxygen and carbon, were considered (Bukhari et al., 2021).

Atomic Force Microscope (AFM)

An AFM (Broker; Germany) imaging technique was employed to analyze the synthesis of CuNPs using *R. stricta*. The reported morphology of CuNPs was found to be influenced by the

shape of the probe, specifically in relation to its lateral dimensions. The height measurements possess the capability to accurately and precisely determine the elevation of nanoparticles. The CuNPs biosynthesized from *R. stricta* exhibited an average diameter of 42.21 nm and an average roughness of 11.18 nm (figure 6).

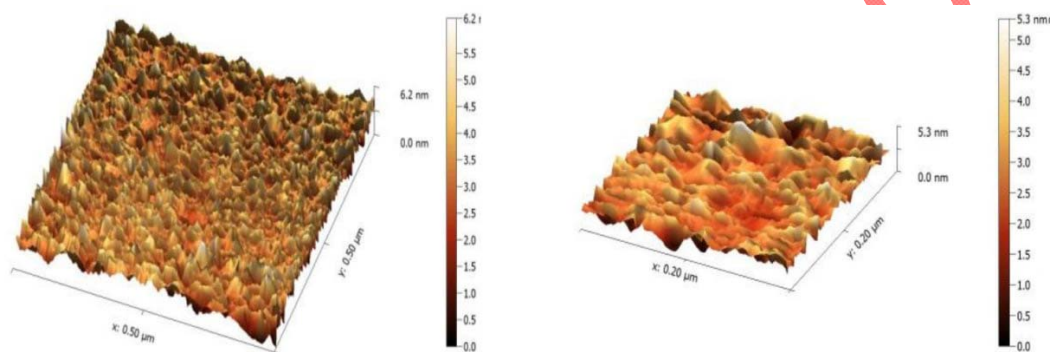


Figure (6) AFM analysis shows three-dimension images, and topography of biogenic CuNPs synthesis by *R. stricta*

X-Ray Diffraction (XRD) Analysis

The XRD analysis revealed that the average crystallite size of CuNPs synthesized using *R. stricta* was determined to be 15.95 nm (figure 7).

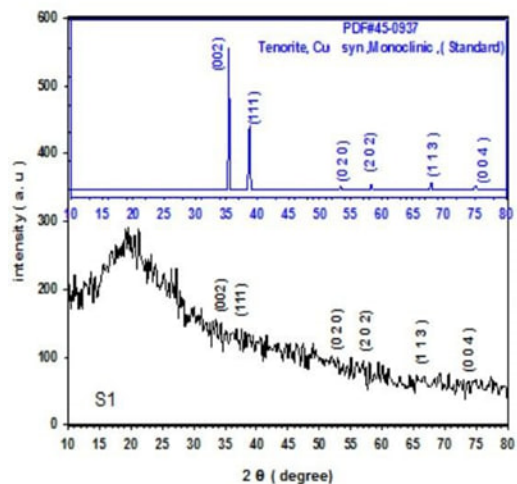


Figure (7) XRD pattern and quantitative analysis of the sample CuNPs as synthesized by *R. stricta*.

Zeta potential of CuNPs

As shown in Figure 8, zeta potential of the synthesized CuNPs was 42 mV. In this regard, zeta potential is considered an important indicator for the stability of a colloid, since the magnitude of the zeta potential expresses the extent of the electrostatic repulsion between the same species constituting that colloid. The value of 42 mV indicates that the prepared nanoparticles exhibit a good stability (Mali et al., 2020).

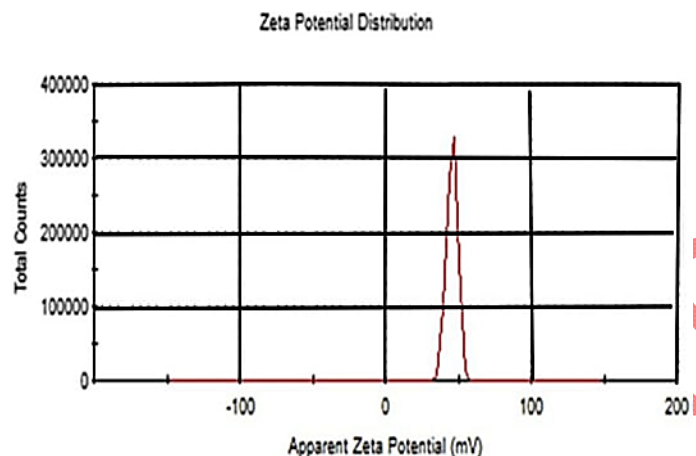


Figure 8. Zeta potential of the synthesized CuNPs at 42 mV.

Wound Healing Rate (%)

During the first to the fourth week of the research period, the healing rate of the wounded rabbits with *S. aureus* increased gradually ($P < 0.05$). It varied significantly across the experimental treatments (Table 1).

Table 1: The effects of CuNPs and Fusidic acid on the rate of wound healing (percent) of rabbits weekly.

Treatment groups	1 st week	2 nd week	3 rd week	4 th week
Group A (control)	31.00±1.68Dc	45.75±0.95Cc	63.00±1.97Bc	76.50±2.82Ac

(No.5)				
CuNPs-treated group (No.5)	52.25±1.59Da	74.00±1.87Ca	90.50±0.74Ba	100.75±1.41Aa
Fusidic acid-treated group (No.5)	33.50±1.42Db	53.25±3.45Cb	69.25±2.96Bb	91.50±2.31Ab

The differences in capital letters horizontally refer to the mean existence of significant values at (P<0.05).
The differences in small letters vertically refer to the mean existence of significant values at (P<0.05).

Small letters indicated that: Means within the same column bearing different letters are significantly different at (P < 0.05).

The highest rate of healing was seen in the CuNPs-treated group (100.75±1.41), followed by the Fusidic acid (Xa-Bc-Biotech; China) - treated group (91.50±2.31). For the duration of the study, treatment CuNPs performed the best in terms of healing rate (1st week to 4th week). These findings suggest that copper nanoparticles expedite the healing of wounds.

Healing Time

Throughout the study period, Table (2) displayed the healing time needs (in days) of the various treatments. The findings from the study revealed a statistically significant difference between experimental treatments (P<0.05). During the course of treatment, no adverse effects were seen in terms of the animal's body weight, overall health, or behavior.

Table 2: The effects of CuNPs and Fusidic acid on the rabbit's wound healing time at 4th week.

Treatment groups	Healing time (Days)
Group (control) (No. 5)	32.00±0.40A
CuNPs-treated group (No. 5)	16.25±0.47C
Fusidic acid -treated group (No. 5)	22.25±0.75B

The differences in capital letters vertically refer to the mean existence of significant values at (P < 0.05).

Figure (9) shows images of the groups of infected wounds treated with CuNPs for 0, 7, 14, and 21 days. Significantly, after 7 days of treatment, CuNPs successfully reduced the size and inflammation of the infected wound. Re-epithelialization is vital in wound healing as the skin performs a significant barrier function in protecting the body against pathogens (Zou et al., 2021).



Figure 9 : (A) Digital images of wound healing taken on various days (0, 7, 14, and 21).

After 3 and 7 days, the untreated, infected wounds of the control groups displayed significant inflammation (figure 10).



Figure 10: Wounds infected in the control groups

Hematological analysis

The WBC count of the various treatments studied was significantly affected by the experimental groups ($P < 0.05$), as shown in Table 3. The present study demonstrated that the WBC count was considerably increased in the non-treated/control group (at 0 and 28 days) compared to the treated group. Nevertheless, the treated group rebounded at 14-, 21-, and 28-day intervals, with the 7-day interval showing the greatest increase.

Capital letters indicated that: Means within the same row bearing different letters are significantly different at ($P < 0.05$).

Small letters indicated that: Means within the same column bearing different letters are significantly different at ($P < 0.05$).

Table 3: The effects of CuNPs and Fusidic acid on the Total number of white blood cells (cells/ μ l) in rabbits at weekly intervals.

Treatment groups	0 days	1 st week	2 nd week	3 rd week	4 th week
Group A (control) (No. 5)	6700 \pm 40.86 Ea	10775 \pm 46.46 Da	1100 \pm 45.49 Ca	11500 \pm 51.02 Ba	11700 \pm 43.69 Aa
CuNPs- treated group (No. 5)	5800 \pm 46.26 Da	9000 \pm 39.02 Ac	8200 \pm 52.31 Bc	7400 \pm 49.27 Cb	6000 \pm 39.46 Db
Fusidic acid treated group) (No. 5)	6100 \pm 45.26 Da	10300 \pm 47.51 Ab	9500 \pm 47.37 Bb	7600 \pm 34.26 Cb	6300 \pm 41.48 Db

The differences in capital letters horizontally refer to the mean existence of significant values at ($P < 0.05$).
The differences in small letters vertically refer to the mean existence of significant values at ($P < 0.05$).

Bacterial counts

All of the treatment groups that received either CuNPs or Fusidic acid were shown to inhibit the development of the bacteria *S. aureus* successfully. The results indicate that CuNPs-treated group could eradicate all bacterial cell-infected wounds in 7 days, whereas Fusidic acid-treated group could eradicate all bacterial cell-infected wounds in 12 days (Table 4). This confirmed that CuNPs are a more effective antibacterial agent.

Table 4: Bacterial Count Prior to and Following Treatment.

Treatment Groups	Day	Bacterial count CFU/10 _μ l
Group Control (+) (No. 5)	3	1.4×10 ¹⁰ CFU
	7	3.3×10 ⁹ CFU

	9	6×10^9 CFU
CuNPs-treated group (No. 5)	3	4.2×10^5 CFU
	7	0 CFU
	9	0 CFU
	12	0 CFU
	14	0 CFU
Fusidic acid-treated group (No. 5)	3	6.2×10^5 CFU

	7	5.1×10^5 CFU
	9	4.1×10^5 CFU
	12	0 CFU
	14	0 CFU

* Analysis reveals statistically significant differences ($P < 0.001$) on days 3, 7, 9, 12, and 14 between the CuNPs, Fusidic acid and control groups.

Histological examination

The stained sections of healing wounds from the control group, the group treated with Fusidic acid, and the group treated with CuNPs on various days are presented in the following. The examination was conducted using H&E stain at a magnification of 400x.

On the third day in the control group, it was observed that there was a loss of normal skin architecture with the absence of the epidermis. Also, the gap was filled with granulation tissue formation, accompanied by the infiltration of inflammatory cells. The sections that were stained in fusidic acid-treated wounds exhibited a greater infiltration of inflammatory cells and the deposition of edematous material, with a limited presence of fibroblasts. However, the group treated with CuNPs exhibited a lower level of inflammatory cell infiltration in comparison to the group treated with Fusidic acid. Additionally, the presence of superficial necrotic tissue, along with edematous deposition and a limited number of fibroblasts, was observed (figure 11).

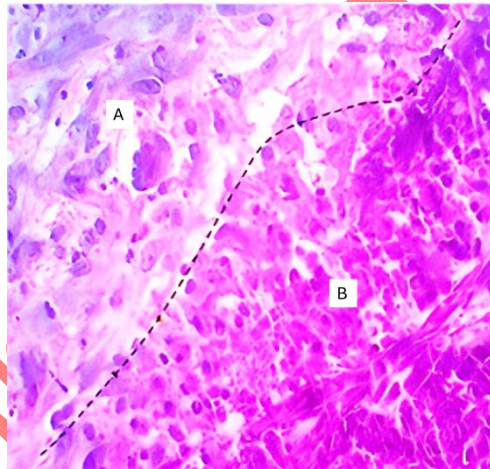


Figure 11 –A : Histopathological characteristics of cutaneous wounds on day 3 in untreated. Control group at incision line show demarcation line (dotted line) between (A)normal skin tissue and (B) granulation tissue with sever Inflammatory cell (Black arrow)

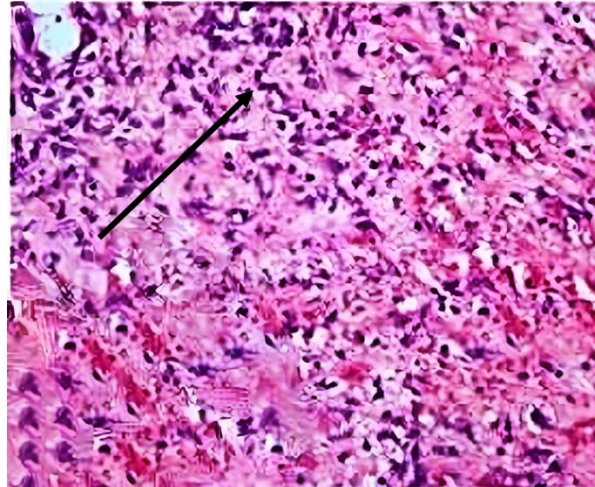


Figure 11 –B : Histopathological characteristics of cutaneous wounds on day 3 fusidic acid-treated groups exhibited a greater infiltration of inflammatory cells and the deposition of edematous material, with a limited presence of fibroblasts.

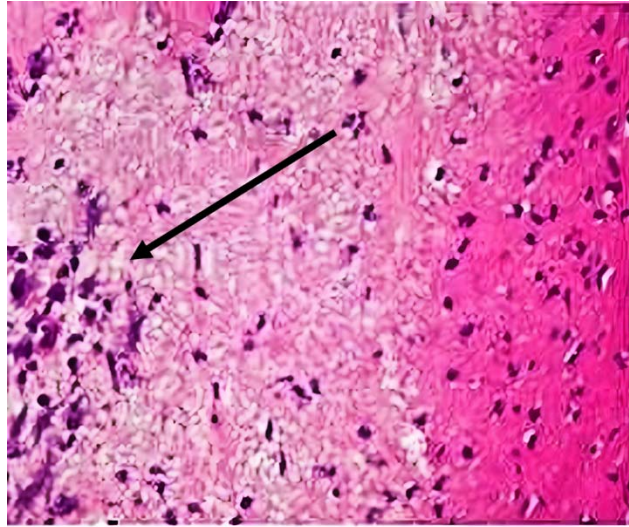


Figure 11 –C : Histopathological characteristics of cutaneous wounds on day 3 CuNPs-treated groups .exhibited a lower level of inflammatory cell infiltration in comparison to the group treated with Fusidic acid

On the seventh day, the wound sections of the control group exhibited a notable presence of inflammatory cells, suggesting that the inflammatory response remained uncontrolled. This could be attributed to the lack of antibacterial efficacy in the treatments administered. A notable inflammatory response was observed in the group that received treatment with Fusidic acid, which was accompanied by an increase in fibroblast proliferation. The experimental group that received CuNPs exhibited a mild inflammatory response, which was accompanied by an augmented proliferation of fibroblasts (figure 12).

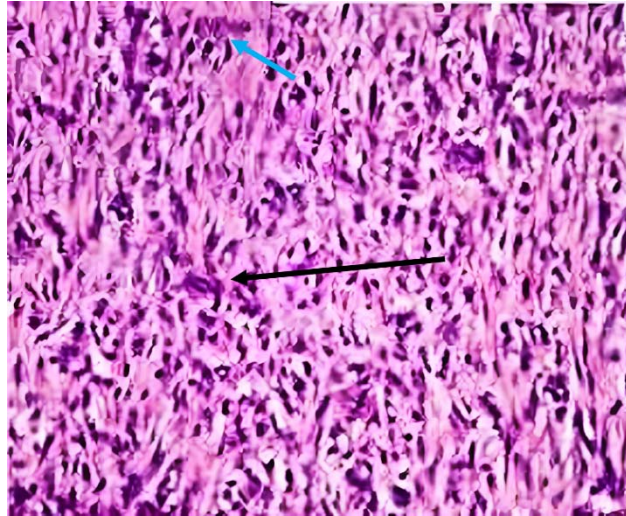


Figure 12 –A : Histopathological characteristics of cutaneous wounds on day 7 in untreated, Fibroblast (Black arrow); blood vessels (Blue arrow)

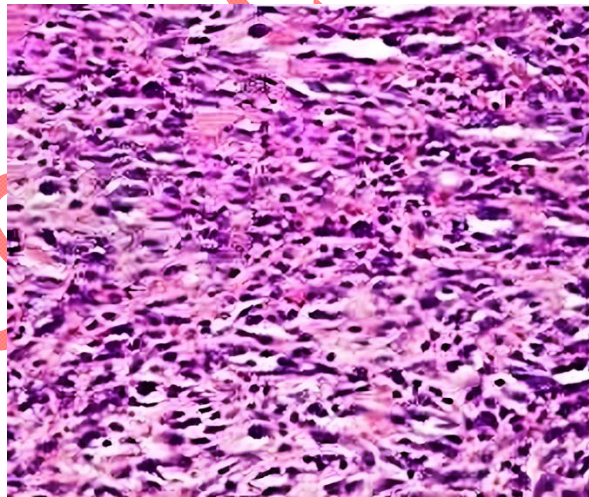


Figure 12 –B : Histopathological characteristics of cutaneous wounds on day 7 in Fusidic Acid-treated groups

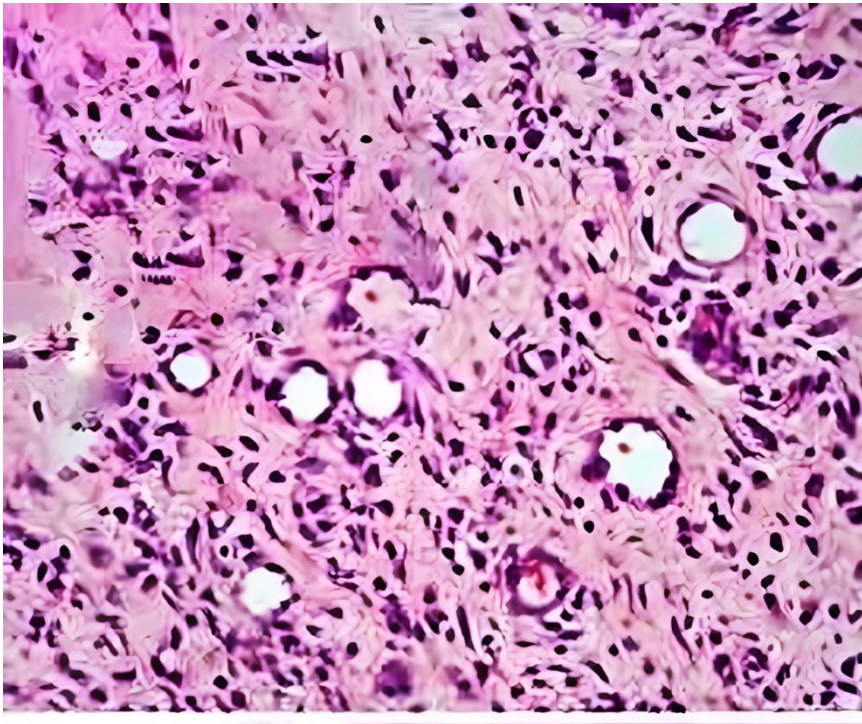


Figure 12 –C : Histopathological characteristics of cutaneous wounds on day 7 in CuNPs-treated groups

On the tenth day, the control group exhibited a substantial presence of inflammatory cells and an unhealed wound. The observations within the group administered with Fusidic acid demonstrated resemblances to those within the control group. On the other hand, the group

subjected to CuNPs demonstrated noteworthy fibroblast proliferation and the formation of well-organized blood vessels, concomitant with collagen deposition (figure 13).

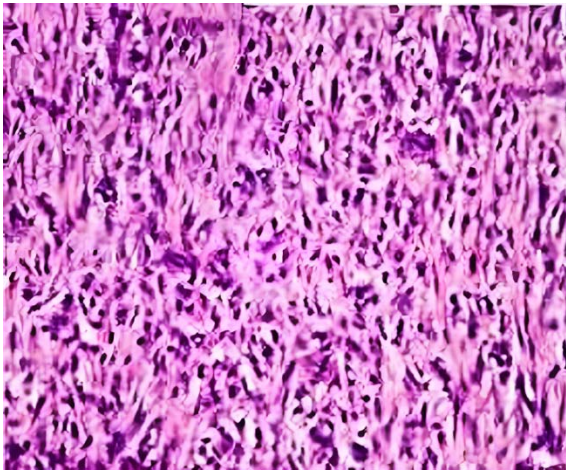


Figure 13 –A : **Histopathological characteristics of cutaneous wounds on day 10 in untreated groups**

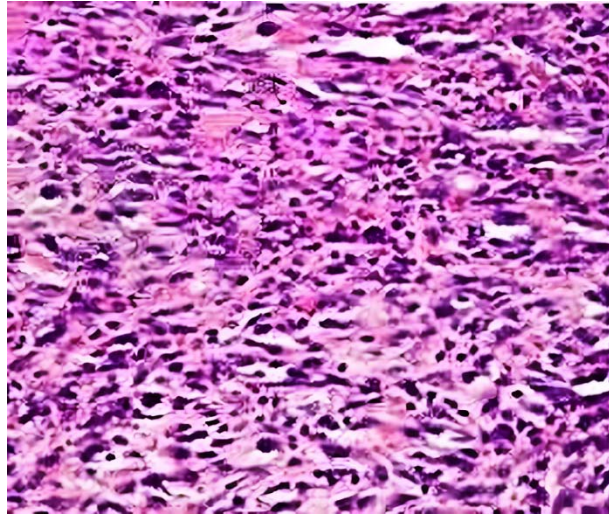


Figure 13 –B : **Histopathological characteristics of cutaneous wounds on day 10 in fusidic acid groups**

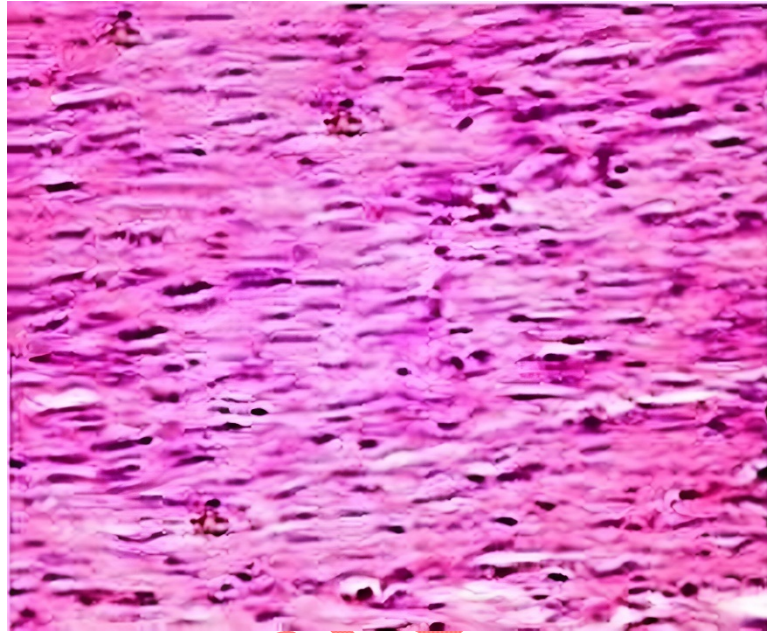


Figure 13 –C : Histopathological characteristics of cutaneous wounds on day 10 in CuNPs-treated groups

On the fourteenth day, the control group demonstrated a significant presence of inflammatory cells, despite the absence of epithelial layer formation. On the other hand, the wounds that were treated with Fusidic acid and CuNPs demonstrated the formation of a complete superficial epithelial layer along with the presence of well-established granulation tissue. The experimental group that received copper nanoparticles (CuNPs) demonstrated a more pronounced and mature superficial epithelial layer when compared to the group that received Fusidic acid. Additionally, a notable observation was made regarding the organization of

collagen fibers in the group subjected to CuNPs treatment, which exhibited a significantly higher degree of organization in comparison to the remaining groups (figure 14).

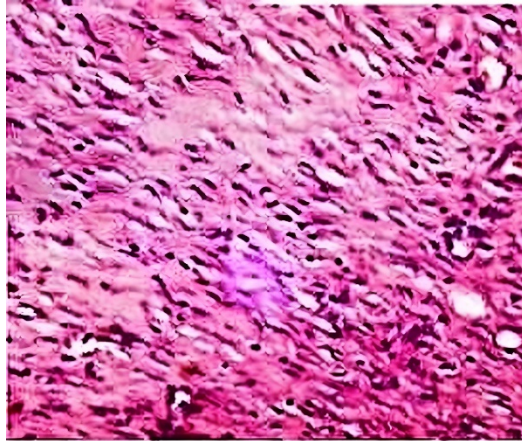


Figure 14 –A : Histopathological characteristics of cutaneous wounds on day 14 in untreated groups.

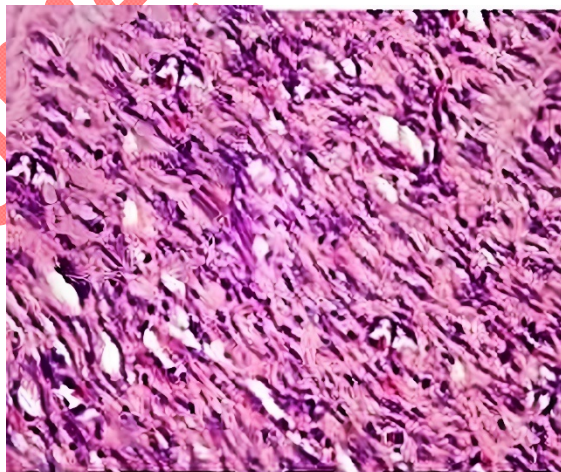


Figure 14 –B : Histopathological characteristics of cutaneous wounds on day 14 in fusidic acid, treated groups.

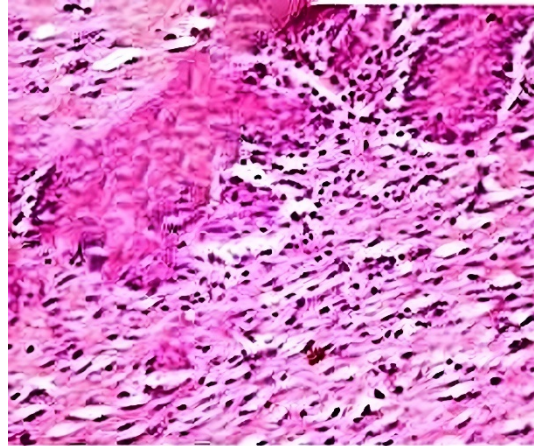


Figure 14 –C : Histopathological characteristics of cutaneous wounds on day 14 in CuNPs-treated groups.

Discussion

The process of wound healing poses a significant challenge to researchers in the field. The process of wound healing commences with an initial inflammatory response, which is subsequently succeeded by the proliferation and migration of dermal and epidermal cells, as well as the synthesis of matrix components. These events collectively aim to bridge the wound gap and restore the integrity of the skin barrier (Alizadeh et al., 2019). In conclusion, the processes of tissue remodeling and differentiation facilitate a near-complete restoration of skin tissue and the reestablishment of its aesthetic properties (Hussain et al., 2022). According to (Wassif et al.,

2021), the implementation of local therapy can effectively facilitate the healing process and mitigate the occurrence of systemic side effects.

Wound contraction is a biological process in which cells strategically arrange the extracellular matrix (ECM) of their surrounding tissue to expedite the healing process by minimizing the quantity of ECM that must be generated. Wound contraction offers several advantages, primarily by expediting the healing process through the reduction of granulation tissue production required for tissue replacement (Zhang et al., 2022).

Considering the abovementioned, the assessment of wound contraction serves as a crucial method for determining the advancement of healing in cutaneous wounds. The observed increase in wound contraction in rabbits treated with CuNPs in the current study can be attributed to several factors, including enhanced fibroblast proliferation, increased collagen synthesis, and improved epithelialization. While the wound size reduction was observed in both the Fusidic acid-treated group and the CuNPs-treated group, the CuNPs-treated group exhibited a more pronounced effect. This suggests that CuNPs have a greater potential for enhancing the healing of cutaneous wounds compared to Fusidic acid.

According to a study conducted by (Tao et al., 2019), the application of CuNPs resulted in a significant reduction in the wound surface area in rabbits within the first day. The contraction data observed within the 7–10-day timeframe demonstrated that CuNPs play a significant role in the proliferative phase as well.

The presence of inflammation in rabbits is commonly observed following a bacterial infection, resulting in an elevation of white blood cell count. The immune response of the host functions as a defensive mechanism that effectively combats bacterial invasion. The rise in white blood cells has been associated with the development of an infection caused by pathogenic bacteria, which in turn triggers the immune system to generate defensive cells. The significance of these cells in the body's immune response lies in their capacity to release immune chemicals that facilitate the eradication of microorganisms (Salem et al., 2020; Hossieni et al., 2021).

The groups treated with Fusidic acid and CuNPs exhibited non-significant numbers of WBCs when infected with *S. aureus*. This suggests that CuNPs have a positive effect in counteracting the negative impact of bacteria and restoring the WBC count to normal levels.

S. aureus is a bacterium that belongs to the gram-positive category and is characterized by its anaerobic nature. The organism is widely acknowledged as a prominent causative agent of cutaneous infections, presenting a considerable risk to the overall well-being of the general population. The ability of *S. aureus* to endure oxidative substances plays a significant role in its ability to persist. Organisms in the logarithmic growth phase demonstrate a notable capacity to tolerate oxidative byproducts. The emergence of bacterial resistance in *S. aureus* presents significant obstacles in the management of infections attributed to this particular pathogen. The implementation of a preclinical animal model for *S. aureus* that is both efficient and cost-effective could offer an additional avenue for assessing the efficacy of antimicrobial agents (Treffon et al., 2020; Moradifar et al., 2024).

The pathogenic bacteria can be effectively inhibited through the utilization of CuNPs, owing to their capacity to traverse the bacterial cell membrane unhindered due to their small dimensions. This penetration of the cell membrane subsequently results in the degradation of essential components such as minerals, proteins, and genetic material, ultimately leading to the demise of the bacterial cell. Moreover, it has been observed that CuNPs exhibit a potent antibacterial effect. Nevertheless, it is important to note that an excessive buildup of these nanoparticles can lead to the demise of microbial cells (Gkanatsiou et al., 2019; Al-Garawi et al., 2022).

The utilization of the antibiotic fusidic acid, known for its wide-ranging antibacterial properties (Liu et al., 2020), likely leads to the inhibition of *S. aureus* and consequently promotes accelerated wound healing with no residual scarring observed in the group treated with fusidic acid. In contrast to the control groups, the wounds that were treated with CuNPs or antibiotics exhibited the formation of a new layer of skin starting from day 3, and the healing process was concluded by day 14, as reported by (Rafi et al., 2023). The study conducted by (Rafi et al., 2023) assessed wound healing by evaluating various factors including re-epithelialization, infiltration of inflammatory cells, regeneration and arrangement of collagen, as well as the presence of granulation tissue and skin appendages.

Metal NPs typically infiltrate bacterial cells through an adsorption mechanism, leading to the release of metal ions that cause DNA damage and the generation of reactive oxygen species (ROS) NPs. This process results in a substantial increase in the surface area of bacterial cells, which subsequently interacts with intracellular enzymes (Abdelghany et al., 2023). The

biopolymer is composed of carboxyl and amine groups, while copper typically forms interactions with these functional groups present on the surface of bacterial cells. The antibacterial efficacy of CuNPs is attributed to their ionic nature and surface charge. These nanoparticles effectively interact with various functional groups present on the cell surface, as discussed by (Guan et al., 2021).

Conclusions

Based on the findings of this study, the utilization of *R. stricta* leaves extract for the biosynthesis of CuNPs is demonstrated to be a straightforward, environmentally sustainable, efficient, and economically viable method of synthesis. Nano copper has the potential to serve as an alternative therapeutic approach for treating wounds that are infected with *S. aureus*. This is due to the demonstrated ability of CuNPs to facilitate the healing process by exerting antibacterial and anti-inflammatory effects. At the histological level, it was observed that the group treated with CuNPs exhibited a more rapid healing process characterized by complete re-epithelialization of the epidermis, significant fibroblastic activity, formation of dermal granulation tissue rich in collagen, and minimal infiltration of inflammatory cells.

ACKNOWLEDGEMENTS

The authors express their gratitude for the ethical support provided by the Veterinary Medicines/ University of Kufa, Iraq.

CONFLICTS OF INTEREST

There is no conflict of interest.

AUTHORS' CONTRIBUTION

The authors mentioned have significantly and directly contributed to the research and have provided their consent for its publication.

FUNDING

No external funds were received to complete this study.

References

- Abdelghany, T. M., Al-Rajhi, A. M. H., Yahya, R., Bakri, M. M., Al Abboud, M. A., Yahya, R., Qanash, H., Bazaid, A. S., & Salem, S. S. (2023). Phytofabrication of zinc oxide nanoparticles with advanced characterization and its antioxidant, anticancer, and antimicrobial activity against pathogenic microorganisms. *Biomass Conversion and Biorefinery*, 13(1), 417–430. <https://doi.org/10.1007/s13399-022-03412-1>
- Alizadeh, S., Seyedalipour, B., Shafieyan, S., Kheime, A., Mohammadi, P., & Aghdami, N. (2019). Copper nanoparticles promote rapid wound healing in acute full thickness defect via acceleration of skin cell migration, proliferation, and neovascularization. *Biochemical and Biophysical Research Communications*, 517(4), 684–690. <https://doi.org/10.1016/j.bbrc.2019.07.110>
- Al-Mousaw, M., Bustani, G. S., Barqaawee, M. J. A., & AL-Shamma, Y. M. (2022, January). Evaluation of histology and sperm parameters of testes treated by lycopene against cyclophosphamide that induced testicular toxicity in Male rats. In *AIP Conference Proceedings*, Vol. 2386, No. 1 . <https://doi.org/10.1063/5.0067059>

- Al-Garawi, N. A. H. D., Suhail, A. A., Kareem, H. A., & Bustani, G. S. (2022). Study of Lipid Profile and Leptin hormone and Adiponectin hormone hypertensive patients in Najaf Governorate. *Revista Electronica de Veterinaria*, 45-51.
- Awwad, A. M., Salem, N. M., & Abdeen, A. O. (2013). Green synthesis of silver nanoparticles using carob leaf extract and its antibacterial activity. *International Journal of Industrial Chemistry*, 4(1), 1–6. <https://doi.org/10.1186/2228-5547-4-29>
- Badri, A., Slimi, S., Guergueb, M., Kahri, H., & Mateos, X. (2021). Green synthesis of copper oxide nanoparticles using Prickly Pear peel fruit extract: Characterization and catalytic activity. *Inorganic Chemistry Communications*, 134, 109027. <https://doi.org/10.1016/j.inoche.2021.109027>
- Behera, S. S., Nath, I., Nayak, S., Parija, S. C., Mishra, U. K., Kundu, A. K., Panda, S. K., Mishra, S. R., & Behera, M. (2019). Histomorphological Study of Cutaneous Wound Healing in Rabbits Using Xenogenic Adipose Derived Stem Cells. *Journal of Animal Research*, 9(5), 645–652. <https://doi.org/10.30954/2277-940X.05.2019.3>
- Bukhari, S. I., Hamed, M. M., Al-Agamy, M. H., Gazwi, H. S. S., Radwan, H. H., & Youssif, A. M. (2021). Biosynthesis of copper oxide nanoparticles using *Streptomyces* MHM38 and its biological applications. *Journal of Nanomaterials*, 2021, 1–16. <https://doi.org/10.1155/2021/6693302>
- Bustani, G., & Kashef Alghetaa, H. (2024). Exploring the Impact of Aryl Hydrocarbon Receptor (AhR) Modulation on the Blood-Testis Barrier Integrity via Tight Junction Protein-1 function. *Iranian Journal of Veterinary Medicine*, (), -. doi: 10.22059/ijvm.2024.374259.1005541

- Cardoso, C. G., Ayer, I. M., Jorge, A. T., Honsho, C. S., & Mattos-Junior, E. (2020). A comparative study of the cardiopulmonary and sedative effects of a single intramuscular dose of ketamine anesthetic combinations in rabbits. *Research in Veterinary Science*, 128, 177–182. <https://doi.org/10.1016/j.rvsc.2019.11.016>
- Caroling, G., Tiwari, S. K., Ranjitham, A. M., & Suja, R. (2013). Biosynthesis of silver nanoparticles using aqueous broccoli extract-characterization and study of antimicrobial, cytotoxic effects. *Asian J Pharm Clin Res*, 6(4), 165–172. <https://journals.innovareacademics.in/index.php/ajpcr/article/view/520> .
- Chinnathambi, A., Awad Alahmadi, T., & Ali Alharbi, S. (2021). Biogenesis of copper nanoparticles (Cu-NPs) using leaf extract of *Allium noeanum*, antioxidant and in-vitro cytotoxicity. *Artificial Cells, Nanomedicine, and Biotechnology*, 49(1), 500–510. <https://doi.org/10.1080/21691401.2021.1926275>
- Diniz, F. R., Maia, R., Rannier Andrade, L., & Andrade, L. N. (2020). Vinicius Chaud M., da Silva CF, Correa CB, de Albuquerque RLC, da Costa LP, Shin SR, et al. Silver Nanoparticles-Composing Alginate/Gelatine Hydrogel Improves Wound Healing in Vivo. *Nanomaterials*, 10, 390. <https://doi.org/10.3390/nano10020390>
- Foroutan, S., Eslampour, M. A., Emaneini, M., Jabalameli, F., & Akbari, G. (2022). Characterization of Biofilm Formation Ability, Virulence Factors and Antibiotic Resistance Pattern of *Staphylococcus aureus* Isolates from Subclinical Bovine Mastitis. *Iranian Journal of Veterinary Medicine*, 16(2), 144-154. doi: 10.22059/ijvm.2021.323994.1005174
- Gaddafi, M. S., Yakubu, Y., Junaidu, A. U., Bello, M. B., Bitrus, A. A., Musawa, A. I., Garba, B., & Lawal, H. (2023). Occurrence of Methicillin-resistant *Staphylococcus aureus* (MRSA) From

Dairy Cows in Kebbi, Nigeria. *Iranian Journal of Veterinary Medicine*, 17(1), 19-26. doi: 10.22059/ijvm.17.1.1005256

Gkanatsiou, C., Karamanoli, K., Menkissoglu-Spiroudi, U., & Dendrinou-Samara, C. (2019). Composition effect of Cu-based nanoparticles on phytopathogenic bacteria. Antibacterial studies and phytotoxicity evaluation. *Polyhedron*, 170, 395–403. <https://doi.org/10.1016/j.poly.2019.06.002>

Guan, G., Zhang, L., Zhu, J., Wu, H., Li, W., & Sun, Q. (2021). Antibacterial properties and mechanism of biopolymer-based films functionalized by CuO/ZnO nanoparticles against *Escherichia coli* and *Staphylococcus aureus*. *Journal of Hazardous Materials*, 402, 123542. <https://doi.org/10.1016/j.jhazmat.2020.123542>

Hasanin, M., Al Abboud, M. A., Alawlaqi, M. M., Abdelghany, T. M., & Hashem, A. H. (2021). Ecofriendly synthesis of biosynthesized copper nanoparticles with starch-based nanocomposite: antimicrobial, antioxidant, and anticancer activities. *Biological Trace Element Research*, 1–14. <https://doi.org/10.1007/s12011-021-02812-0>

Huimin, X., Xin, C., Xuanzhe, L., Gen, W., & Yu, Y. (2023). Recent advances in decellularized biomaterials for wound healing. *Materials Today Bio*, 100589. <https://doi.org/10.1016/j.mtbio.2023.100589>

Hussain, Z., Thu, H. E., Rawas-Qalaji, M., Naseem, M., Khan, S., & Sohail, M. (2022). Recent developments and advanced strategies for promoting burn wound healing. *Journal of Drug Delivery Science and Technology*, 68, 103092. <https://doi.org/10.1016/j.jddst.2022.103092>

- Hossieni, M., Kiani, S. J., Tavakoli, A., Kachooei, A., Habib, Z., & Monavari, S. H. (2024). In Vitro Inhibition of Rotavirus multiplication by Copper Oxide Nanoparticles. *Archives of Razi Institute*, 79(1), 83-91 .<https://doi.org/10.32592/ARI.2024.79.1.83>
- Islam, F., Shohag, S., Uddin, M. J., Islam, M. R., Nafady, M. H., Akter, A., Mitra, S., Roy, A., Emran, T. Bin, & Cavalu, S. (2022). Exploring the journey of zinc oxide nanoparticles (ZnO-NPs) toward biomedical applications. *Materials*, 15(6), 2160. <https://doi.org/10.3390/ma15062160>
- Liu, L., Shen, X., Yu, J., Cao, X., Zhan, Q., Guo, Y., & Yu, F. (2020). Subinhibitory concentrations of fusidic acid may reduce the virulence of *S. aureus* by down-regulating sara and saers to reduce biofilm formation and α -toxin expression. *Frontiers in Microbiology*, 11, 25. <https://doi.org/10.3389/fmicb.2020.00025>
- Mali, S. C., Dhaka, A., Githala, C. K., & Trivedi, R. (2020). Green synthesis of copper nanoparticles using *Celastrus paniculatus* Willd. leaf extract and their photocatalytic and antifungal properties. *Biotechnology Reports*, 27, e00518. <https://doi.org/10.1016/j.btre.2020.e00518>
- Mirnezami, M., Rahimi, H., Fakhar, H. E., & Rezaei, K. (2018). The Role of Topical Estrogen, Phenytoin, and Silver Sulfadiazine in Time to Wound Healing in Rats. *Ostomy/Wound Management*, 64(8), 30–34. PMID: 30212362. <https://doi.org/10.26855/ijcemr.2023.04.023>
- Moradifar, N., Moayyedkazemi, A., Mohammadi, H., Ahmadi, S., & Raziani, Y. (2024). Investigating the potential application of organic and inorganic nanoparticles for gastric cancer treatment: an evidence-based review. *Archives of Razi Institute*, 79(2), 264-271.

- Pal, M., Shuramo, M. Y., Tewari, A., Srivastava, J. P., & HD, C. (2023). Staphylococcus aureus from a Commensal to Zoonotic Pathogen: A Critical Appraisal. <https://doi.org/10.1016/j.mtcomm.2023.105914>
- Rafi, R., Zulfqar, S., Asad, M., Zeeshan, R., Zehra, M., Khalid, H., Akhtar, N., & Yar, M. (2023). Smart wound dressings based on carbon doped copper nanoparticles for selective bacterial detection and eradication for efficient wound healing application. *Materials Today Communications*, 35, 105914. <https://doi.org/10.1016/j.mtcomm.2023.105914>
- Rahman, H., Rauf, A., Khan, S. A., Ahmad, Z., Alshammari, A., Alharbi, M., Alam, A., & Suleria, H. A. R. (2023). Green Synthesis of Silver Nanoparticles Using *Rhazya stricta* Decne Extracts and Their Anti-Microbial and Anti-Oxidant Activities. *Crystals*, 13(3), 398. <https://doi.org/10.3390/cryst13030398>
- Rahchamani, R., Zarooni, S., & Borhani, M. S. (2024). The Chemical Composition and Antibacterial Effect of Essential Oils of Rosemary and Basil in Milk. *Iranian Journal of Veterinary Medicine*, (), -. doi: 10.22059/ijvm.2024.372443.1005517
- Raja, S., Ramesh, V., & Thivaharan, V. (2017). Green biosynthesis of silver nanoparticles using *Calliandra haematocephala* leaf extract, their antibacterial activity and hydrogen peroxide sensing capability. *Arabian Journal of Chemistry*, 10(2), 253–261. <https://doi.org/10.1016/j.arabjc.2015.06.023>
- Rani, R., Sharma, D., Chaturvedi, M., & Yadav, J. P. (2020). Green synthesis of silver nanoparticles using *Tridax procumbens*: their characterization, antioxidant and antibacterial activity against MDR and reference bacterial strains. *Chemical Papers*, 74, 1817–1830. <https://doi.org/10.1007/s11696-019-01028-w>

- Razdan, K., Garcia-Lara, J., Sinha, V. R., & Singh, K. K. (2022). Pharmaceutical strategies for the treatment of bacterial biofilms in chronic wounds. *Drug Discovery Today*, 27(8), 2137–2150. <https://doi.org/10.1016/j.drudis.2022.04.020>
- Salem, M. I., El-Sebai, A., Elnagar, S. A., El-hady, A., & Mohamed, A. (2020). Evaluation of lipid profile, antioxidant and immunity statuses of rabbits fed *Moringa oleifera* leaves. *Animal Bioscience*. <https://doi.org/10.5713/ab.20.0499>
- Samuel, M. S., Ravikumar, M., John J, A., Selvarajan, E., Patel, H., Chander, P. S., Soundarya, J., Vuppala, S., Balaji, R., & Chandrasekar, N. (2022). A review on green synthesis of nanoparticles and their diverse biomedical and environmental applications. *Catalysts*, 12(5), 459. <https://doi.org/10.3390/catal12050459>
- Sato, H., Ebisawa, K., Takanari, K., Yagi, S., Toriyama, K., Yamawaki-Ogata, A., & Kamei, Y. (2015). Skin-derived precursor cells promote wound healing in diabetic mice. *Annals of Plastic Surgery*, 74(1), 114–120 <https://doi.org/10.1097/SAP.0000000000000342>
- Tanideh, N., Rokhsari, P., Mehrabani, D., Samani, S. M., Sarvestani, F. S., Ashraf, M. J., Hosseinabadi, O. K., Shamsian, S., & Ahmadi, N. (2014). The healing effect of licorice on *Pseudomonas aeruginosa* infected burn wounds in experimental rat model. *World Journal of Plastic Surgery*, 3(2), 99. PMC4236996
- Tao, B., Lin, C., Deng, Y., Yuan, Z., Shen, X., Chen, M., He, Y., Peng, Z., Hu, Y., & Cai, K. (2019). Copper-nanoparticle-embedded hydrogel for killing bacteria and promoting wound healing with photothermal therapy. *Journal of Materials Chemistry B*, 7(15), 2534–2548. <https://doi.org/10.1111/cmi.13158>

- Treffon, J., Chaves-Moreno, D., Niemann, S., Pieper, D. H., Vogl, T., Roth, J., & Kahl, B. C. (2020). Importance of superoxide dismutases A and M for protection of *Staphylococcus aureus* in the oxidative stressful environment of cystic fibrosis airways. *Cellular Microbiology*, 22(5), e13158. <https://doi.org/10.1111/cmi.13158>
- Vinelli, A., Primiceri, E., Brucale, M., Zuccheri, G., Rinaldi, R., & Samorì, B. (2008). Sample preparation for the quick sizing of metal nanoparticles by atomic force microscopy. *Microscopy Research and Technique*, 71(12), 870–879. <https://doi.org/10.1002/jemt.20631>
- Wassif, R. K., Elkayal, M., Shamma, R. N., & Elkheshen, S. A. (2021). Recent advances in the local antibiotics delivery systems for management of osteomyelitis. *Drug Delivery*, 28(1), 2392–2414. <https://doi.org/10.1080/10717544.2021.1998246>
- Yaşayan, G., Nejati, O., Ceylan, A. F., Karasu, Ç., Ugur, P. K., Bal-Öztürk, A., Zarepour, A., Zarrabi, A., & Mostafavi, E. (2023). Tackling chronic wound healing using nanomaterials: advancements, challenges, and future perspectives. *Applied Materials Today*, 32, 101829. <https://doi.org/10.1016/j.apmt.2023.101829>
- Zhang, Q., Wang, P., Fang, X., Lin, F., Fang, J., & Xiong, C. (2022). Collagen gel contraction assays: From modelling wound healing to quantifying cellular interactions with three-dimensional extracellular matrices. *European Journal of Cell Biology*, 101(3), 151253. <https://doi.org/10.1016/j.ejcb.2022.151253>
- Zhang, S., Lin, L., Huang, X., Lu, Y.-G., Zheng, D.-L., & Feng, Y. (2022). Antimicrobial properties of metal nanoparticles and their oxide materials and their applications in oral biology. *Journal of Nanomaterials*, 2022. <https://doi.org/10.1155/2022/2063265>

- Zhang, W., Chou, X., Shi, T., Ma, Z., Bao, H., Chen, J., Chen, L., Li, D., & Xue, C. (2017). Measurement Technology for Micro-Nanometer Devices. John Wiley & Sons. ISBN-10 : 9781118717967
- Zhao, H., Maruthupandy, M., Al-mekhlafi, F. A., Chackaravarthi, G., Ramachandran, G., & Chelliah, C. K. (2022). Biological synthesis of copper oxide nanoparticles using marine endophytic actinomycetes and evaluation of biofilm producing bacteria and A549 lung cancer cells. Journal of King Saud University-Science, 34(3), 101866. <https://doi.org/10.1016/j.jksus.2022.101866>
- Zou, M.-L., Teng, Y.-Y., Wu, J.-J., Liu, S.-Y., Tang, X.-Y., Jia, Y., Chen, Z.-H., Zhang, K.-W., Sun, Z.-L., & Li, X. (2021). Fibroblasts: Heterogeneous cells with potential in regenerative therapy for scarless wound healing. Frontiers in Cell and Developmental Biology, 9, 713605. <https://doi.org/10.3389/fcell.2021.713605>